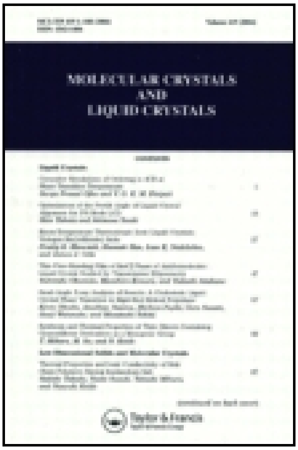

Molecular Crystals and Liquid Crystals Science and Technology. Section A. Molecular Crystals and Liquid Crystals

Publication details, including instructions for authors and subscription information:
http://www.tandfonline.com/loi/gmcl19

Structures and Properties of Induced Lyotropic Cholesteric Phases

Hans-Dieter Dörfler [a], Andrea Göpfert [a] & Carsten Görgens [a]

[a] TU Dresden, Department of Chemistry, D-01062, Dresden, Germany

Version of record first published: 24 Sep 2006

To cite this article: Hans-Dieter Dörfler, Andrea Göpfert & Carsten Görgens (2001): Structures and Properties of Induced Lyotropic Cholesteric Phases, Molecular Crystals and Liquid Crystals Science and Technology. Section A. Molecular Crystals and Liquid Crystals, 367:1, 517-527

To link to this article: http://dx.doi.org/10.1080/10587250108028672

Mol. Cryst. and Liq. Cryst., 2001, Vol. 367, pp. 517-527
Reprints available directly from the publisher
Photocopying permitted by license only

Published by license under the
Gordon and Breach Science Publishers imprint,
a member of the Taylor & Francis Group,
Printed in the USA

Structures and Properties of Induced Lyotropic Cholesteric Phases

HANS-DIETER DÖRFLER, ANDREA GÖPFERT and
CARSTEN GÖRGENS

TU Dresden, Department of Chemistry, D-01062 Dresden, Germany

Phase chirality in disk-like lyotropic cholesteric phases (Ch_D) was investigated, which were induced by center and axial chiral dopants to achiral lyotropic nematic host phases (N_D). In a lyotropic nematic matrix of the N_D phase in the ternary system hexadecyldimethylethylammoniumbromid ($C_{16}Me_2EABr$)/water/n-decanol, a disk-like lyotropic cholesteric phase Ch_D was induced by addition of the axial optically active compound R(-)-1,1′-binaphthalene-2,2′-diyl-hydrogenphosphate (BDP). The *HTP* value of the BDP is generally lower than the *HTP* value of inducing substances with center chirality as cholesterol, prednisolon etc. At constant composition of the N_D phase, the helix lengths were determined in dependence on the BDP concentration by means of evaluation of the "spaghetti-like texture" using polarizing microscopy. The reciprocal helix-lengths are changing linearly with rising BDP concentration. Furthermore selected results of X-ray scattering and diffraction on the structure formation in the Ch_D phase were discussed.

Keywords: Disk-like micelles; textures; helix length; center and axial chirality; X-ray scattering; structures

1. INTRODUCTION

Chirality in liquid crystals, and in science generally, has been the subject of interesting research in the last decades. So lyotropic cholesteric phases have previously been described in the literature [1-39]. Generally, the authors used three-component systems (water, surfactant, cosurfactant) to prepare the lyotropic nematic matrix. Optically active surfactants with different chemical structure have been applied to the formation of lyotropic cholesteric structures.

In the first step the goal of our previous papers [40-47] was to study the lyotropic nematic to lyotropic cholesteric transitions induced by selected chiral dopants. The addition of small amounts of chiral compounds such as cholesterol, d- or l-tartaric acid, lithocholic acid, desoxycholic acid, cholic acid, Na-taurocholate, hydrocortison, prednisolon etc. have been shown to transform lyotropic nematic phases into lyotropic cholesteric phases.

In the next step the aim of these studies was the determination of pitch length from the textures, oriented in magnetic field, and the evaluation of the so called helical twisting power, designed as *HTP* value. Four aspects were important by our following investigations and analysis:

- Characterization of lyotropic cholesteric phase using the axial chiral optically active compound [R(–)-1,1′-binaphthalene-2,2′-diyl-hydrogen-phosphate = BDP] by texture observations and using Small- and Wide-Angle X-ray Scattering (SWAX). Analysis of the structural changes of the micelles in the Ch_D phase in dependence on the BDP concentration.
- Analysis of the influence of the host phase – this means the influence of the composition in the lyotropic nematic matrix – on the properties of the lyotropic cholesteric phase by measurements of the pitch length and by SWAX investigations.
- Comparison of the twisting properties of the center chiral optically compounds with axial chiral optically active compounds.
- Detailed analysis of the main factors for helix formation by evaluation of the structural parameter of the Ch_D phase.

2. RESULTS

2.1. Texture observations and measurements of the helix lengths in dependence on the BDP concentration

The "fingerprint texture" of the non-aligned lyotropic disk-like cholesteric phase Ch_D is shown in Figure 1a. The Ch_D phase is partially oriented under the influence of the glas walls. Neighbouring micellar aggregates will accordingly tend to align so that their long axis are parallel to the interface. This reduces for a given distance the electrostatic repulsion from surface. In analogy to the lyotropic nematic phases the corresponding lyotropic cholesteric phase can also be aligned by a magnetic field.

In the rod-like lyotropic cholesteric phase Ch_C we have found that the helical structure unwinds. The application of an external magnetic field leads to a nematic "Schlieren texture" [40]. In the disk-like cholesteric phase, however, the formation of cholesteric structure can easily be observed by means of polarizing microscopy. As shown in Figure 1a, only one domain of the "fingerprint texture" have an ordered morphology. These domains can be aligned by an external magnetic field. Then, the typical "spaghetti-like texture" is observed as shown in Figure 1b.

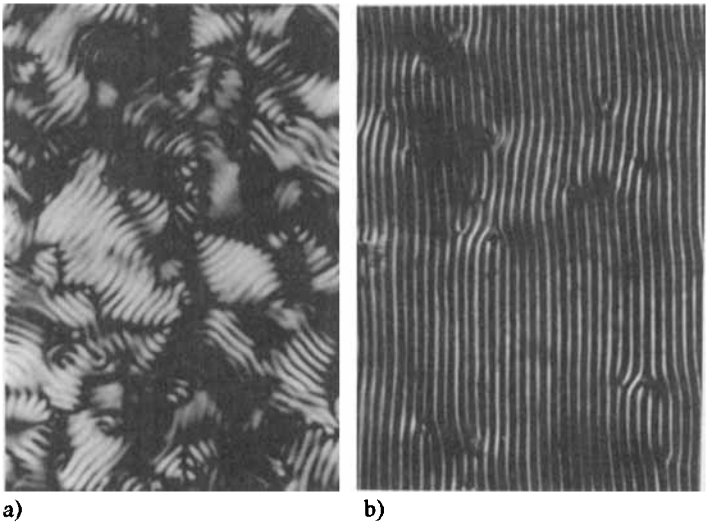

FIGURE 1. Textures of different lyotropic liquid crystals at $T = 298$ K.

a) "Fingerprint texture" of the non-aligned disk-like lyotropic cholesteric phase (Ch_D).

b) "Spaghetti-like texture" of an oriented Ch_D phase. It has been subjected to a magnetic field for 10 h (1,2 tesla)

Magnification 100x. Composition of the quaternary system for the formation of the Ch_D phase: 28wt% $C_{16}Me_2EABr$; 67.7wt% water; 4.3wt% n-decanol; 1.3wt% BDP.

See Color Plate VII at the back of this issue.

A point of special interest in texture observations was the change in pitch length effected by BDP. Figure 2a illustrates the results. At low BDP concentrations the reciprocal pitch length increases linearly. According to

$$HTP = \lim_{c_l \to 0} \frac{1}{p c_l}$$, the HTP values of the optically active compound BDP were calculated with p the helix length, c_l the concentration of BDP and HTP=192,3 mm^{-1} mol^{-1}. This means the HTP value of BDP is very low for instance in comparison to cholesterol, prednisolon etc.

Furthermore we have measured the transition temperatures T^* of the phase transition $Ch_D \rightarrow S$. The results are drawn in Figure 2b. The T^*/c_l curve shows a linear dependence on the BDP concentration.

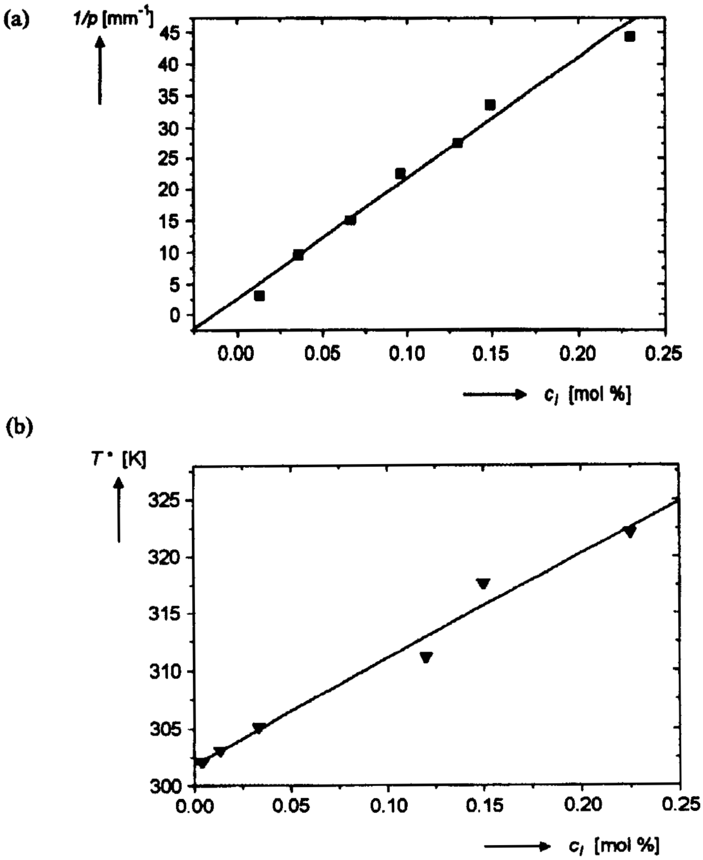

FIGURE 2. (a) Reciprocal pitch length (1/*p*) obtained by evaluating the "spaghetti-like texture" in dependence on the BDP concentration (c_l) at $T = 298$ K.

(b) Temperatures T^* of the phase transition $Ch_D \rightarrow S$ (isotropic phase) in dependence of the BDP-concentration.

Composition of the Ch_D phase: 28 wt % $C_{16}Me_2EABr$; 67.7 wt % water; 4.3 wt % n-decanol; + BDP.

2.2. SWAX measurements and influence of BDP on the structure formation in the Ch_D phase

In Figure 3 are collected some small angle X-ray diffraction patterns of the Ch_D phase in dependence on different BDP concentrations. An interesting feature of the SWAX pattern was that under the condition of parallel X-raying, the (100) and (200) reflexes are not dependend on the BDP concentration. We have not observed a shift of these reflexes. This phenomena was the same, when we have took cholesterol to induce the Ch_D phase [45]. Also the micelle distances shifts not in normal direction. Otherwise under the condition of perpenticular X-raying of the sample, the (010) reflex shifts with increasing BDP concentration to higher values. In Figure 4 these results are summarized.

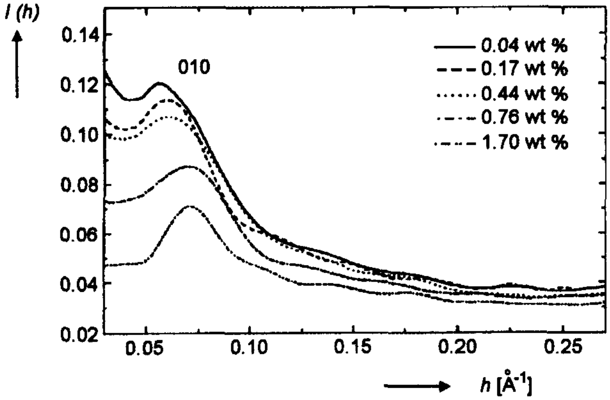

FIGURE 3. Experimental scattering curve (desmeared) of the Ch_D phase under the conditions of the perpendicular X-raying of the sample in dependence on the BDP concentration (c_l in wt %). Composition of the Ch_D phase: 28 wt % $C_{16}Me_2EABr$; 67.7 wt % water; 4.3 wt % n-decanol; + BDP. Symbols: $I(h)$ = scattering intensity; h = scattering vector ($h=(4\pi/\lambda)\sin(\Theta/2)$, λ = wave length of the radiation, Θ = scattering angle).

The aim of the SWAX measurement was to calculate some micelle parameters of the Ch_D phase using the X-ray diffraction curves shown in Figure 3. Details are described in [48]. To calculate the anisotropy of the periodic volume we have measured the SWAX patterns in dependence on different BDP concentrations. The results from the SWAX experiments and of the calculations are summarized in Table 1. From the analysis of the micelle parameters we can conclude that indeed, the solubilization of the BDP molecules into the micelles have took place. The solubilization is connected with a change of the micelle parameters, as to seen in Table 1.

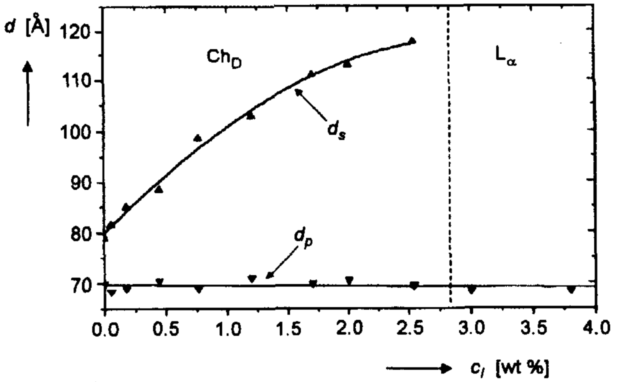

FIGURE 4. Anisotropy ($A = d_s/d_p = d_{010}/d_{100}$) of the periodic volume in dependence on the BDP concentration (c_l) at 298 K under the conditions of the parallel (index p,▼) and perpendicular (index s,▲) X-raying of the sample. Composition of the Ch$_D$ phase: 28 wt % $C_{16}Me_2EABr$; 67.7 wt % water; 4.3 wt % n-decanol. d = Bragg value.

c_l [wt %]	V_P [$10^5 \cdot Å^3$]	V_M [$10^5 \cdot Å^3$]	$A = d_{010}/d_{100}$	$\bar{z}_A$	$\bar{z}_l$	$\bar{z}_M$
0	3.64	1.20	1.17	161	0	–
0.17	3.91	1.29	1.21	172	1	18800
0.44	4.35	1.43	1.27	192	3	6200
0.76	5.09	1.71	1.37	224	6	3800
1.7	6.53	2.26	1.54	284	17	1800
2.0	6.77	2.36	1.58	298	21	1330

TABLE 1 Micelle parameters of the induced Ch$_D$ phase as function of the R(–)-1,1′-binaphthalene-2,2′-diyl-hydrogen-phosphate (BDP) concentration (c_l) at T = 298 K. Composition of the matrix of the N$_D$ phase: 28 wt % $C_{16}Me_2EABr$; 67.7 wt % water; 4.3 wt % n-decanol. Symbols: V_P = periodic volume of the micelle; V_M = micelle volume; $d_{010}/d_{100} = d_s/d_p = A$ = Anisotropy of the periodic volume; $\bar{z}_A$ = average aggregation numbers per micelle; $\bar{z}_l$ = average solubilization numbers of BDP molecules per micelle; $\bar{z}_M$ = average micelle numbers per helix lengths.

The micelle volume rises considerable. We can assume that in the bilayer of the disk-like micelles the optically active compounds probably arrange beside of the surfactant and cosurfactant molecules in the position with the smallest curvature of the micelles. So we can conclude that the distribution of the BDP molecules in the micelles is not homogeneously. Therefore it is to expect that each composition of the micelle interface has its own local concentration profil, changing the curvature of the micelles.

2.3. Influence of the lyotropic nematic host phase on the properties of the lyotropic cholesteric phase

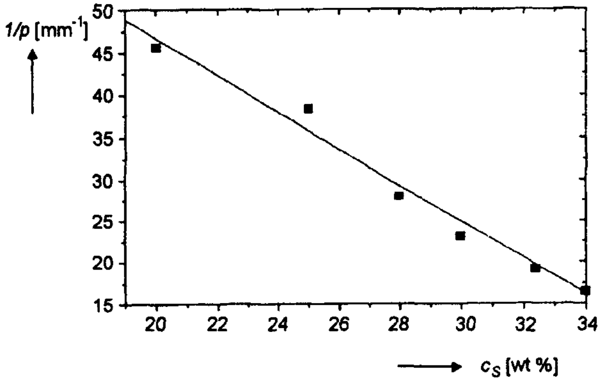

FIGURE 5. Reciproced helix lengths (1/*p*) in dependence on the $C_{16}Me_2EABr$ concentration (c_S) at constant ratio $C_{16}Me_2EABr$/n-decanol = 6.65 and 1.3 wt % BDP at *T* = 298 K.

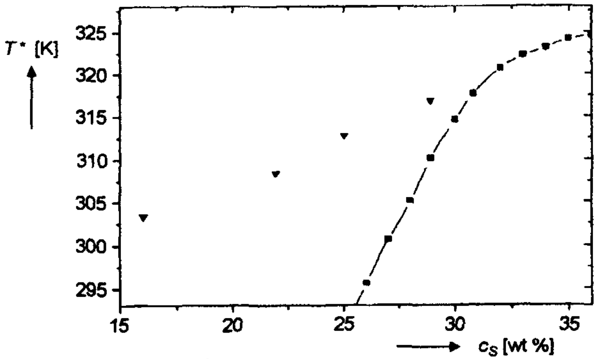

FIGURE 6. Temperatures T^* of the phase transition Ch_D → S (isotropic phase, symbol ▼) and N_D → S (symbol ■) in dependence on the $C_{16}Me_2EABr$ concentration (c_S). Composition of the N_D phase: constant ratio (related to the mass) $C_{16}Me_2EABr$/n-decanol = 6.65. Composition of the Ch_D phase: matrix of N_D phase +1.3 wt % BDP.

As mentioned above after alignment of the Ch_D phase in magnetic field we obtained the so called "spaghetti-like texture" at *T* = 298 K (see Figure 1b). A point of special interest in texture observation was again the change in pitch length effected by changing of the composition of the matrix in the N_D phase. Figure 5 illustrates the results. Similar to Figure 2a, we can see that the reciprocal pitch length increases linearly with the surfactant concentration c_S.

Again we have measured the temperatures T^* of the phase transition $N_D \rightarrow S$ and $Ch_D \rightarrow S$ in dependence in proportion to the surfactant in the N_D phase and the Ch_D phase. The results are shown in Figure 6. In the upper part of the two curves the increase is linearly but with different slope.

In Figure 7 is drawn Bragg values to demonstrate the anisotropy of the periodic volume as well under the conditions of the parallel and perpenticular X-raying, against the composition of the Ch_D phase. There are differences in the d values. The values of the periodic volumes of the disk-like micelles are in the same order of magnitude.

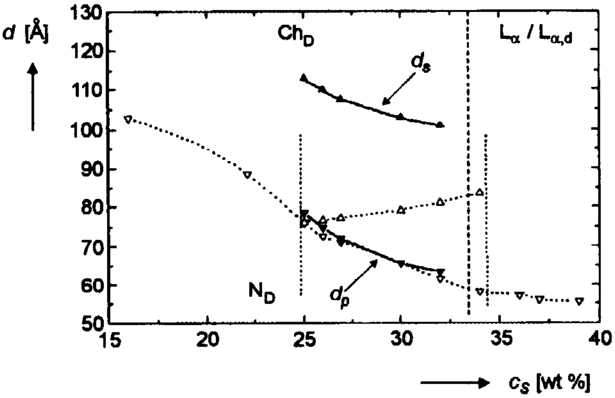

FIGURE 7. Anisotropy ($A = d_s/d_p = d_{010}/d_{100}$) of the periodic volume in the Ch_D phase in dependence on the $C_{16}Me_2EABr$ concentration (c_S) at T = 298 K at a constant ratio (related to the mass) $C_{16}Me_2EABr$/n-decanol and 1.3 wt % BDP. Symbols: d = Bragg values, Ch_D = disk-like lyotropic cholesteric phase; N_D = disk-like lyotropic nematic phase; L_α = lamellar phase, chains fluid; $L_{\alpha,d}$ = lamellar phase with defects; d_s = Bragg values during perpendicular X-raying through the sample; d_p = Bragg-values during parallel X-raying through the sample. Anisotropy A: $A = \frac{d_s}{d_p} = \frac{d_{010}}{d_{100}}$.

In Table 2 are summarized of the different micelle parameters of the Ch_D phase in dependence on the surfactant content at constant surfactant/cosurfactant ratio (= 6.65). The tendency in the micelle parameters is the following: with increasing surfactant concentration the micelle volume and the average aggregation number decrease. The same trends we have observed for the V_P and $\bar{z}_S$ values in the system $C_{16}Me_2EABr$/water/n-decanol/taurocholic acid.

c_S [wt %]	V_P [$10^5 \cdot Å^3$]	V_M [$10^5 \cdot Å^3$]	$A = d_{010}/d_{100}$	$\bar{z}_A$	$\bar{z}_I$
25	7.78	2.35	1.43	314	15.0
27	6.74	2.15	1.52	283	12.2
30	5.52	1.93	1.57	263	10.5
32	5.12	1.76	1.58	240	8.4

TABLE 2 Micelle parameters of the induced $\mathrm{Ch_D}$ phase as function of the $C_{16}Me_2EABr$ concentration (c_S) at constant ratio (related to the mass) $C_{16}Me_2EABr$/n-decanol = 6.65 and 1.3 wt % R(–)-1,1′-binaphthalene-2,2′-diyl-hydrogen-phosphate (BDP). Symbols: V_P = periodic volume of the micelle; V_M = micelle volume; $d_{010}/d_{100} = d_l/d_p = A$ = Anisotropy of the periodic volume; $\bar{z}_A$ = average aggregation numbers per micelle; $\bar{z}_I$ = average solubilization numbers of BDP molecules per micelle.

3. CONCLUSIONS

With our systematic investigations [40–47] about the main parameters and factors for the mechanism of helix formation in a matrix of the disk-like lyotropic nematic phases – details are not written here - we have found out the essential experimental conditions, which are responsible to built up lyotropic cholesteric phases by adding chiral compounds [42–48]. The application of, as well center chiral as axial chiral substances leads in the ternary system surfactant/cosurfactant/water of the lyotropic nematic matrix to the phase transition $\mathrm{N_D} \rightarrow \mathrm{Ch_D}$. Our texture observations and SWAX measurements were very good tools to identify the phases, to measure the helix lengths and to obtaine structural parameters about the micelle size and micelle geometry in the $\mathrm{N_D}$ phase and in the $\mathrm{Ch_D}$ phase.

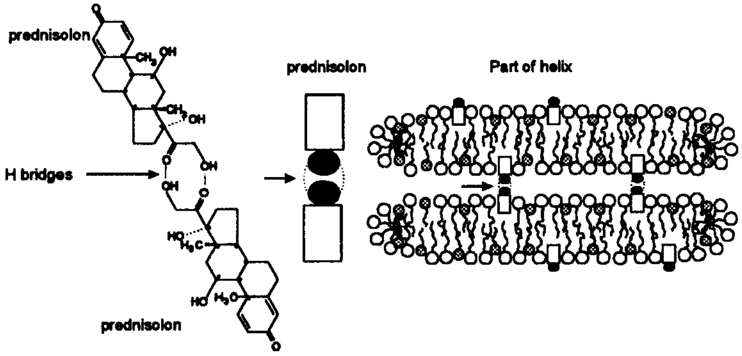

FIGURE 8. Oversimplified model to demonstrate the interaction between two prednisolon molecules arranged in two micelle of the helical stack forming the H bridges.

For the formation of the Ch_D phase and the helices, the solubilization properties of the N_D phase matrix is the importanst factor. The solubilization capacity of the micelles in the N_D phase is strongly dependent on the composition of the N_D phase and on the chemical constitution of the chiral compound. In our experience, the helix formation starts with about 1 – 2 chiral molecules per micelle in the N_D phase. The chiral substances have the properties of cosurfactants. During the incorporation of the chiral substances in the micelles a change in the curvature of the micelles takes place. The chiral compounds are located in such a position, where the micelle have the lessest curvature. The reason for the bond between the disks in the helix is probably the formation of H-bridges between adjacent chiral molecules in the helical stack. The H-bridges between two neighbouring micelles act like a "hinged joint" and bring the two micelles in a fixed position. Afterwards the system has the possibility to form helices. This situation is shown in Figure 8.

References

[1] T. Hashimoto, N. Ouaba, S. Ebisu, H. Kawai *Polym. J. Tokyo* **13**, 897 (1981).
[2] B. Ernst, P. Navard, T. Hashimoto, T. Takeba *Macromolecules* **23**, 1370 (1990).
[3] B.J. Forrest, L.W. Reeves *Chem. Rev.* **81/1**, 1-14 (1981).
[4] Y. Onogi, K. Tokumitsu *Chem. Express* **5**, 201 (1990).
[5] Y. Onogi, T. Okubo *Liq. Cryst.* **12**, 815 (1992).
[6] B. Cai, G. Zhang, F. Wu, H. Gao *Gaofenzi Cailiao Kexue Yu Gouy Cheng* **8**, 71 (1992).
[7] J.Y. Guo, D.G. Gray *Macromolecules* **22**, 2082 (1989).
[8] B.R. Harkness, D.G. Gray *Polym. Prep./Am. Chem. Soc./Div. Polym. Chem.* **31**, 644 (1989).
[9] B.R. Harkness, D.G. Gray *Liq. Cryst.* **8**, 237 (1990).
[10] D. Budgele, D.G. Gray in: *Polymer Fiber Sci.: Recent Adv.*, Ed. Formes, Raymon: 145.
[11] P. Zugenmaier *Papier* **43**, 658 (1990).
[12] M. Siekmeyer, P. Zugenmaier *Cellulose* **347** (1990).
[13] S. Bonazzi, M. Capobianco, M.M. DeMorais, A. Gorbesi, G.M. Gottarelli, P. Marianni, B. Ponzi *J. Am. Chem. Soc.* **113**, 5809 (1991).
[14] G.P. Spada, A. Carcuro, F.P. Colonna, A. Gorbesi, G.M. Gottarelli *Liq. Cryst.* **3**, 651 (1988).
[15] A.S. Tracey, P. Diehl *FEBS Letters* **59**, 131 (1975).
[16] A.M. Figueiredo Neto, Y. Galerne, L. Liebert *J. Phys. Chem.* **89**, 3939 (1985).
[17] B.J. Forrest, L.W. Reeves, M. Vist *Mol. Cryst. Liq. Cryst.* **113**, 37 (1984).
[18] A.S. Tracey, K. Radley *J. Phys. Chem.* **88**, 6044 (1984).
[19] M.R. Alcantara, J.A. Vanin *Mol. Cryst. Liq. Cryst.* **102**, 7 (1984).
[20] G. Melnik, A. Saupe, *Mol. Cryst. Liq. Cryst.* **145**, 95 (1987).
[21] T. Kroin, A.M. Figueiredo Neto, L. Liebert, C. Galerne, *Phys. Rev. A.: Gen. Phys.* **40**, 4667 (1989).
[22] M.R. Alcantara, M.V. de Melo, V.R. Paoli, J.A. Vanin, *J. Coll. Interf. Sci.* **93**, 560 (1993).
[23] A.M. Figueiredo Neto, M.E.M. Helene *J. Phys. Chem.* **91**, 1466 (1987).
[24] M.E.M. Helene, A.M. Figueiredo Neto *Mol. Cryst. Liq. Cryst.* **127**, 1623 (1988).
[25] H. Lee, M.M. Labes *Mol. Cryst. Liq. Cryst.* **44**, 227 (1978).
[26] D. Goldfarbs, M.E. Mosley, M.M. Labes, Z. Luz *Mol. Cryst. Liq. Cryst.* **89**, 119 (1982).
[27] H. Lee, M.M. Labes *Mol. Cryst. Liq. Cryst.* **84**, 137 (1982).

[28] H. Lee, M.M. Labes *Mol. Cryst. Liq. Cryst.* **82**, 335 (1983).
[29] H. Lee, M.M. Labes *Mol. Cryst. Liq. Cryst.* **108**, 125 (1984).
[30] M. DoAido, M.R. Alcantara *Mol. Cryst. Liq. Cryst.* **195**, 45 (1991).
[31] B.J. Forrest, J. Mattai *Chem. Phys. Lipids* **35**, 1 (1984).
[32] M.R. Alcantara, J.A. Vanin *Quimica Nova* **2**, 185 (1986).
[33] B.J. Forrest, L.W. Reeves, M.J. Vist *J. Am. Chem. Soc.* **103**, 690 (1981).
[34] A.S. Tracey, K. Radley *Langmuir* **6**, 1221 (1990).
[35] M.R. Alcantara, M.V. deMelo, V.R. Paoli, J.A. Vanin *Mol. Cryst. Liq. Cryst.* **90**, 335 (1983).
[36] U. Krämer, *Thesis*, Univ. Bayreuth (1990).
[37] M.C. Valente Lopes, A.M. Figueiredo Neto *Phys. Rev.* **A38/2**, 1101 (1988).
[38] M. Acimis, L.W. Reeves *Can. J. Chem.* **58**, 1533 (1980).
[39] K. Radley, A. Saupe *Mol. Phys.* **35**, 1405 (1978).
[40] G. Bartusch, H.-D. Dörfler, H. Hoffmann *Progr. Colloid Polym. Sci.* **89**, 307 (1992).
[41] H.-D. Dörfler, G. Friedrich, C. Swaboda *Tenside Surf. Det.* **32**, 244 (1995).
[42] G. Friedrich, H.-D. Dörfler *Tenside Surf. Det.* **32**, 252 (1995).
[43] H.-D. Dörfler, C. Swaboda *Tenside Surf. Det.* **35**, 18 (1998).
[44] H.-D. Dörfler, C. Swaboda *Tenside Surf. Det.* **35**, 126 (1998).
[45] H.-D. Dörfler, C. Görgens *Tenside Surf. Det.* in press.
[46] H.-D. Dörfler, C. Görgens *Tenside Surf. Det.* in press.
[47] H.-D. Dörfler, C. Görgens *Tenside Surf. Det.* in press.
[48] H.-D. Dörfler, C. Görgens *Tenside Surf. Det.* in press.